Organic Geochemistry 130 (2019) 1–13

Contents lists available at ScienceDirect

Organic Geochemistry

journal homepage: www.elsevier.com/locate/orggeochem

Geochemical assessment of oils from the Mero Field, Santos Basin, Brazil

Ygor dos Santos Rocha [a,b,*], Rosana Cardoso Lopes Pereira [a], João Graciano Mendonça Filho [a,c]

[a] Federal University of Rio de Janeiro (UFRJ), Institute of Geosciences, Av. Athos da Silveira, 274, Prédio do CCMN, Cidade Universitária, 21.949-900 Rio de Janeiro, RJ, Brazil
[b] Division of Geochemistry, PETROBRAS Research and Development Center (CENPES), Av. Horácio Macedo, 950, Cidade Universitária, 21.941-915 Rio de Janeiro, RJ, Brazil
[c] Palynofacies and Organic Facies Laboratory (LAFO)/DEGL/IGEO/CCMN/UFRJ, Av. Athos da Silveira, 274 – Prédio do CCMN, Sala JI-020, Cidade Universitária, 21.941-916 Rio de Janeiro, RJ, Brazil

ARTICLE INFO

Article history:
Received 21 November 2018
Received in revised form 20 January 2019
Accepted 23 January 2019
Available online 24 January 2019

Keywords:
FT-ICR MS
Polar compounds
Petroleomics
Crude oil
Santos basins
Pre-salt
Lacustrine oils
Biomarkers

ABSTRACT

Three crude oils recovered from three different wells of the Mero Field in the pre-salt of the Santos Basin were selected for detailed geochemical analysis. The samples were analyzed using a 7.2 T LTQ FT-ICR MS instrument by negative electrospray ionization (–ESI), focusing on the polar compounds, i.e., nitrogen-, sulfur-, and oxygen-containing compounds (NSO). Additionally, a combination of traditional geochemical methods including GC-FID, GC-MS, and carbon isotopic composition (whole oil and *n*-alkanes) were used to assess the samples. Through this work, it was demonstrated that –ESI FT-ICR MS is a reliable method for assessing crude oil composition and providing information about the origin and thermal maturity of the samples. Results showed that the dominant heteroatom classes are N_1, O_2, N_1O_1, and O_1. Due to the similarity of double bound equivalent (DBE), which means number of unsaturation present in an organic molecule, and carbon number distributions for the N_1 class species it is possible to suggest that Mero's filling history had an oil charge representing the peak of the oil window (0.7–0.9 %Ro) and that the oils were generated by a source rock deposited in a lacustrine environment.

1. Introduction

According to the Brazilian Petroleum Agency (ANP), the Libra Area, offshore Santos Basin (Fig. 1), has estimated recoverable oil volumes of between eight to twelve billion barrels in Neobarremian to Aptian carbonate reservoirs (coquinas, grainstones, and stromatolites) (Carlotto et al., 2017). The Libra consortium led by Petrobras with a 40% interest also consists of partners Shell (20%), Total (20%), CNPC (10%) and CNOOC Limited (10%). The Production Sharing Agreement is managed by the state-owned company Pré-Sal Petróleo SA (PPSA) and the first appraisal well (3-RJS-731-RJ) located in the northwest sector confirmed the high hydrocarbon producing potential of the area (Carlotto et al., 2017).

Geochemical assessments of crude oil samples are typically carried out to identify their origin (depositional environment), infer the thermal evolution of their source rocks and to evaluate possible post-accumulation alterations such as biodegradation. Crude oils consist predominantly of hydrocarbon compounds, such as paraffin, cycloalkanes and aromatic hydrocarbons (~85%), followed by polar compounds (~15%), such as nitrogen-, sulfur-, oxygen-containing compounds (NSO compounds). Even though NSO compounds are present in a smaller concentrations in crude oils, they can be used to assess hydrocarbon generation, migration, and alteration mechanisms.

Han et al. (2018) summarized the application Fourier transform ion cyclotron resonance mass spectrometry (FT-ICR MS), for the analysis and study of heteroatomic compounds with higher molecular weights (m/z > 330 Da) that are not possible by conventional gas chromatography-mass spectrometry (GC/MS) methods. The most commonly investigated NSO compounds using conventional GC-MS analyses are carbazoles, thiophenes, phenols, and derivatized carboxylic acids.

The ultrahigh mass resolution and accuracy of FT-ICR MS are ideal for the analysis of complex heteroatomic compounds, allowing for the assignment of detected masses to chemical formulas (Marshall et al., 2007). When coupled with the electrospray ionization technique (ESI), which produces pseudo-molecular ions, the detailed composition of selective polar species can be resolved (Qian et al., 2001). Ultrahigh resolution mass spectrometry has characterized thousands of hydrocarbon and polar species in petroleum and related products. Recently, Smith et al. (2018) showed that a 21 T FT-ICR MS was capable of assigning approximately 49,000 molecular formulas in the ESI negative mode for a Canadian bitumen. This approach has enabled "petroleomics", the comprehensive characterization of petroleum at the molecular level

* Corresponding author at: Division of Geochemistry, PETROBRAS Research and Development Center (CENPES), Av. Horácio Macedo, 950, Cidade Universitária, 21.941-915 Rio de Janeiro, RJ, Brazil.
E-mail address: ygor.rocha@petrobras.com.br (Y.S. Rocha).

https://doi.org/10.1016/j.orggeochem.2019.01.011
0146-6380/

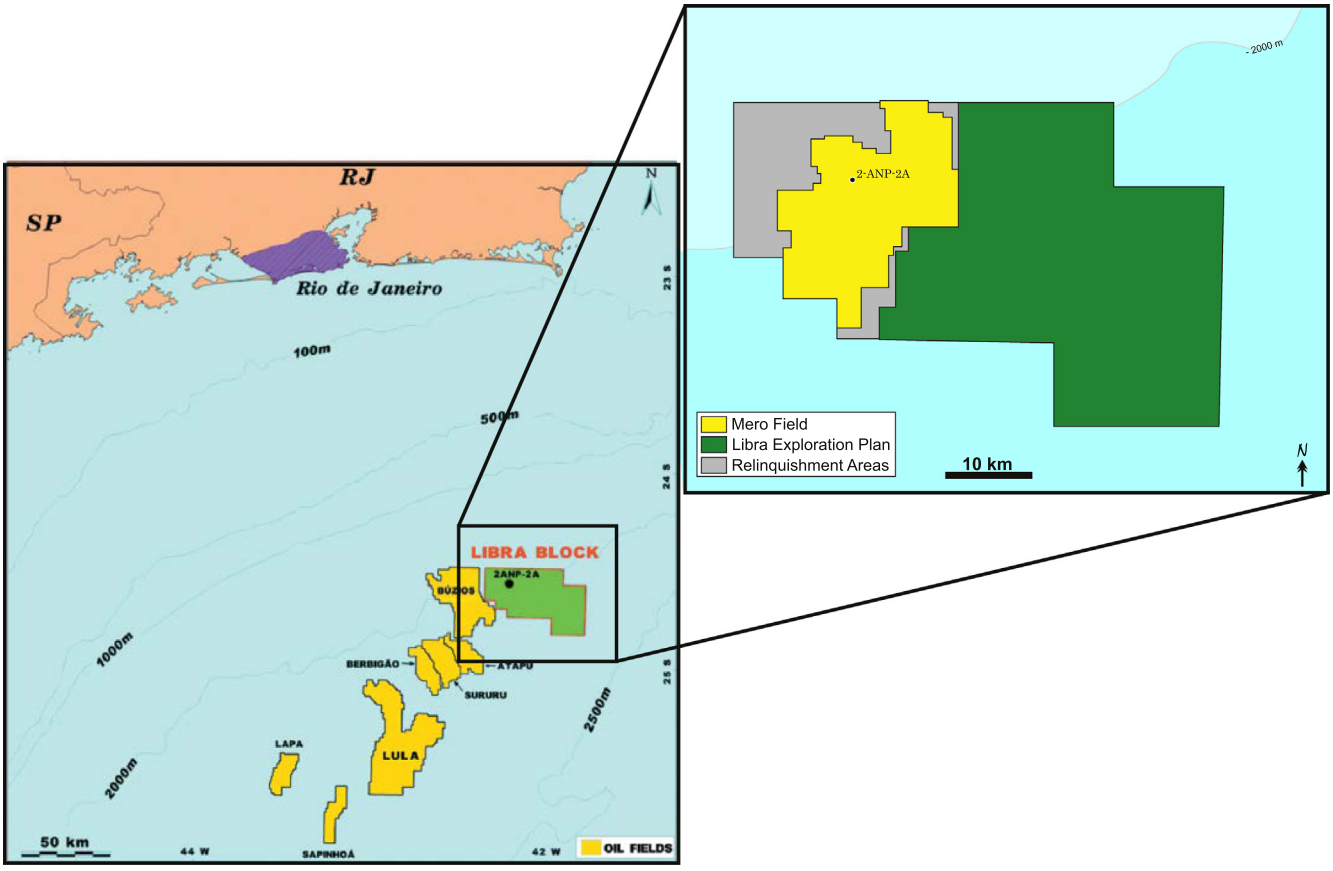

Source: Modified from Carloto (2017) and Petrobras

Fig. 1. Santos Basin location map and Mero's ring fence.

(Rodgers et al., 2005) allows for predictions of chemical properties and behavior (Marshall and Rodgers, 2004). While molecular structures are still to be defined, this technology has provided insight into the distributions of polar species that can be applied to research throughout the entire oil industry chain. Studies from oil generation to refining processes represent a link between upstream and downstream activities.

The distribution of nonhydrocarbon compounds in petroleum was employed in many studies to differentiate sources and to identify compositional changes during biodegradation, expulsion and migration fractionation, and thermal maturity evolution (e.g., Hughey et al., 2004; Vaz et al., 2013; Oldenburg et al., 2014, 2017; Poetz et al., 2014; Mahlstedt et al., 2016; Wan et al., 2017; Han et al., 2018a, 2018b; Ziegs et al., 2018; Ji et al., 2018; Rocha et al., 2018a, 2018b).

In a recent study, Rocha et al. (2018a) used a combination of traditional geochemical methods and –ESI FT-ICR MS to characterize and assess the depositional environments of different oil families recovered from four different basins from the Brazilian marginal coast. They demonstrated that kerogen type plays an important role in the heteroatomic composition of the analyzed crude oils. Such characteristics resulted in a clear difference between marine and lacustrine-derived oils based on polar species generated from Type I and Type II kerogens. The dominant species in the studied crude oils is N_1, followed by O_1, O_2, and N_1O_1 with remarkable differences between marine and lacustrine origins. Lacustrine oils are enriched in Nx (nitrogen-bearing) compounds, while marine oils are dominated by Ox (oxygen-bearing) compounds. These characteristics enabled us to create several polar compound ratios that can be used to assess the depositional environment of oil samples.

In a related study, Rocha et al., 2018b evaluated the impact of the level of thermal maturity on polar compounds using hydrous pyrolysis (HP). The HP experiments were performed under isothermal conditions for 72 h at eleven different temperatures (300, 310, 320, 325, 330, 340, 345, 350, 355, 360 and 365 °C) to simulate the full range of thermal maturity from early bitumen to maximum oil generation (Spigolon et al., 2015). Compositional changes in the evolved polar species were characterized by –ESI FT-ICR MS. Several new thermal maturity parameters covering the full range of oil generation based on systematic changes in the acidic O_2 species were developed.

In this study, we apply our learnings to a real world petroleum system. Three Mero Field crude oils were analyzed using selected polar compounds assessed by –ESI FT-ICR MS associated with traditional geochemical parameters to evaluate their source input, depositional environments, and thermal maturity.

2. Geological background

The Santos Basin was formed during the opening of the central segment of the South Atlantic Ocean in the Early Cretaceous. The discovery of a giant oil province composed by the pre-salt in the Brazilian southeastern margin led to several industrial and academic studies (Chaboureau et al., 2013; Carlotto et al., 2017; Tedeschi et al., 2017; Chafetz et al., 2018; Pietzsch et al., 2018).

The stratigraphic record can be divided into three main supersequences: rift, post-rift, and drift (Moreira et al. 2007). The rift supersequence comprises volcanic rocks, continental siliciclastics, and interbedded lacustrine coquinas and organic-rich shales of the Itapema Formation. In distal settings, the overlying post-rift

supersequence comprises interbedded carbonates and shales of the Barra Velha Formation. The post-rift supersequence comprises of evaporites with predominantly anhydrite and halite and locally with more soluble salts such as carnallite, sylvite, and tachyhydrite of the Ariri Formation (Tedeschi et al., 2017).

Pietzsch et al. (2018) described that a sequence of marine platform carbonates lies above these pre-salt formation that are overlain by thick deposits of coastal, shelf, slope and pelagic sediments, ranging in age from Albian to the Holocene. The stratigraphic chart of the Santos Basin along with its biostratigraphic zones, with a focus on the specific interval corresponding to the Early Cretaceous is published in Pietzsch et al. (2018) (their Fig. 2). The Mero reservoirs are Aptian carbonates from the Guaratiba Group (Carlotto et al., 2017). In the 2-ANP-2A discovery well, the coquinas and carbonates from the Itapema and Barra Velha formations are both in the oil generation and preservation window. Fluid sampling of the 2-ANP-2A well recovered 27 °API gravity oil with a gas to oil ratio (GOR) ranging between 375 and 448 scf/stb, CO_2 content ranging between 38 and 42% and less than 0.5 to 16 ppm of H_2S.

3. Samples and methods

3.1. Samples

Three oil samples recovered from flash liberation tests (pressure-volume-temperature or PVT sampling) from three different wells located in the Mero Field (Fig. 1) were selected for the analyses described below. Due to the proprietary nature of these samples, the well names was codified and are denominated as Well A, B and C. All the samples were collected from the carbonates reservoirs of the Barra Velha Fm. The wells are distributed in different parts of the field.

3.2. GC-FID and GC-MS analysis

Approximately 50 mg of each crude oil sample was diluted in 1 mL of dichloromethane and analyzed by GC-FID. The GC-FID analyses were performed with an Agilent Technologies 7890B gas chromatograph (GC) equipped with a split/splitless injector, a fused silica DB-5 phenyl/methyl polysiloxane capillary column (30 m × 0.25 mm × 0.25 μm) and a flame ionization detector (FID). The oven temperature was programmed from 40 °C to 320 °C with a heating rate of 2.5 °C/min. High-purity helium was used as a carrier gas at a constant flow of 1.3 mL/min.

Approximately 60 mg of each crude oil sample was weighed, dissolved in *n*-hexane, and spiked with an appropriate quantity of the internal standard β -cholane. After homogenization, the mixture was injected into a Margot Köhnen-Willsch (MKW) semi-automated medium pressure liquid chromatography (MPLC) instrument to obtain the corresponding saturated hydrocarbon fractions. The aromatic, resin, and asphaltene fractions are also obtained but only the saturated hydrocarbons were used for biomarker analysis.

Analysis of the saturated fractions by gas chromatograph coupled to mass spectrometry (GC/MS) was performed on an Agilent 7890B GC equipped with a split/splitless injector and interfaced to an Agilent 5977A quadrupole mass selective detector. The separation was achieved by injecting the mixture into a DB-5 fused silica capillary column (60 m × 0.25 mm × 0.25 μm). The GC oven was temperature-programmed from 55 °C as an initial temperature (held for 2 min) to 150 °C at 20 °C/min, followed by a second gradient of 1.5 °C/min to a final temperature of 320 °C (held for 20 min). Aliquots of 1 μL of the saturated hydrocarbon fraction were injected into the GC system in the splitless mode. High-purity helium was used as the carrier gas under a constant flow mode at a rate of 1.6 mL/min. The mass spectrometer was operated in the electron impact (EI) mode at 70 eV, at a source temperature of 230 °C and a quadrupole temperature of 150 °C. The samples were analyzed in a selected ion monitoring (SIM) mode. The concentrations of selected biomarkers relative to the whole oil sample were determined by comparing the peak areas in the selected ions chromatogram to that of the internal standard β-cholane. Response factors for the components of interest relative to the internal standard were assumed to be 1.0.

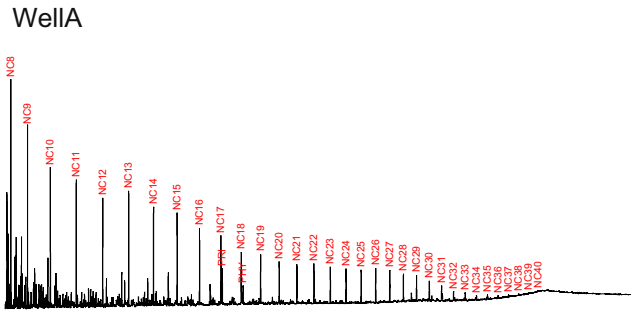

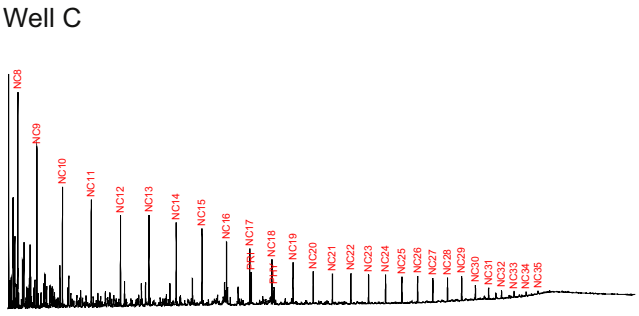

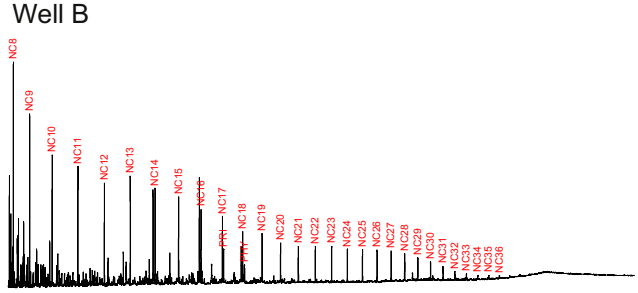

Well	Pr/Ph	Pr/nC17	Ph/nC18	CPI	°API
A	1.97	0.51	0.35	1.04	27.53
B	1.80	0.51	0.37	1.02	28.19
C	1.89	0.58	0.38	1.04	27.79

Fig. 2. Whole oil gas chromatograms and main ratios of crude oils recovered from Mero Field.

3.3. Carbon isotopic analysis

The carbon isotopic composition analysis of the whole oil samples was performed on a ThermoFisher Scientific Flash EA 1112 elemental analyzer (Flash EA 1112) coupled to Delta Plus XL isotope ratio mass spectrometer for isotope ratios (**Delta Plus XL**) via a ConFlo II combustion interface. The stable carbon isotopic ratios of *n*-alkanes were determined using a 7890 gas chromatograph (Agilent Technologies) coupled to a Delta V Plus mass spectrometer via a GCC III interface (ThermoFisher Scientific). A 30 m × 0.25 mm i.d. DB-1 (film thickness 0.25 μm) capillary column was used. The GC temperature program for *n*-alkane separation ramped from 40 to 190 °C (1 min) at 20 °C/min, then to 320 °C (10 min) at 3 °C/min. Ultrahigh purity helium was used as a carrier gas with a constant flow rate of 1.3 mL/min. Each sample was injected in the on-column mode. For isotopic standardization, a CO_2 reference gas was automatically introduced into the isotopic ratio mass spectrometer in a series of pulses at the beginning and the end of each analysis. Prior to carbon isotope analyses, the CO_2 reference gas was calibrated relative to Vienna Pee Dee Belemnite (VPDB). Instrument performance was routinely checked using *n*-alkane standard mixes with known $\delta^{13}C$ values (*n*-C_{16} – *n*-C_{30} provided by Indiana University). Precision for replicate measurements of the standard *n*-alkanes is typically up to 0.50‰. Isotopic compositions are reported as $\delta^{13}C$ values relative to VPDB and represent at least the average of duplicate measurements.

3.4. ESI FT-ICR MS analysis

Mass spectrometry analyses were performed in the negative ion ESI mode using a 7.2 T LTQ FT ultra-mass spectrometer (ThermoScientific, Bremen, Germany). Crude oil samples (1 mg) were dissolved in 1 mL of toluene and then diluted with 1 mL of methanol containing 0.1% of ammonium hydroxide. All solvents used for sample preparation were HPLC grade and purchased from Sigma-Aldrich. Samples were loaded into a 500 μL Hamilton syringe for direct infusion into the LTQ FTMS. The general ESI conditions were as follows: spray voltage of 3.5 kV, tube lens voltage of −140 V, and a flow rate of 5 μL/min. Mass spectra consisted of over 100 microscans processed via the Xcalibur 2.0 software (ThermoScientific, Bremen, Germany).

3.5. Data processing

Data processing was performed using the Petro MS software developed by Petrobras and UNICAMP (State University of Campinas) for formula attribution and a recalibration of a known homologous series from the measured *m*/*z* values of polar crude oil compounds. Elemental formulas were calculated and assigned based on the *m*/*z* values within an error range of 1 ppm. For each spectrum, an automated analysis was used to assign formulas to peaks with a signal-to-noise ratio greater than 3. The selected elements were ^{12}C, ^{13}C, ^{1}H, ^{16}O, ^{14}N, ^{32}S, and ^{34}S. Data analysis and visualization were performed using the Ragnarök software (Aphorist Inc.), which is a data processing software tool that visualizes and interprets multidimensional and multisample FT-ICR MS data. Apart from the determination of molecular masses and double bond equivalents [DBE comes from (CcHhNnSsOo) = c − h/2 + n/2 + 1] of detectable individual species in whole oils or bitumen fractions, the Ragnarök software also grouped abundances of whole heteroatom classes (a heteroatom class is a group of compounds with a uniform heteroatom population), DBE distributions within a heteroatom class, and carbon number distributions for all the attributed compounds. A variety of cross plots, and ternary diagrams were used to interpret the results.

4. Results and discussion

4.1. Conventional geochemical characteristics

The oil samples showed a set of common characteristics (Table 1), such as high wax contents, comprising a full range of $C_8 - C_{35}$ normal alkanes (*n*-alkanes) and isoprenoids such as pristane (Pr) and phytane (Ph). The carbon preference index (CPI) values were 1.02–1.04, with a very slight odd/even *n*-alkane dominance (Fig. 2). These numbers agree with other lacustrine oils from the Brazilian continental basins (Mello et al., 1988) and could indicate that the oils are thermally mature (Peters et al., 2005). The oils are not biodegraded as evident by the preservation of the C_6-C_{12} *n*-alkanes, the absence of unresolved complex mixture (UCM) and no loss of saturates components (Fig. 2).

The distribution of saturated biomarkers indicates the oils (Fig. 3) reveals that they are related to the same generation pod due to the homogeneous biomarker pattern. Conventional geochemical parameters from the saturated biomarkers (Peters et al., 2005; Dembicki, 2016) such as the hopane/sterane ratio, tetracyclic polyprenoids (TPP) ratio (TPP/TPP + diasteranes, measured at *m*/*z* 259), and steranes distribution, show that those oils have typical features of lacustrine-derived oils.

Additionally, they show a strong correlation with organic extracts from source rocks deposited during the Jiquiá Stage (Itapema Formation) that is described as the main source rock from the Santos Basin (data not shown).

To evaluate further whether the oil samples were expelled from the same organic facies, the carbon isotope compositions for each of the individual *n*-alkanes, ranging from C_{10}-C_{33}, were measured. Pedentchouk and Turich (2017) summarized the main controls on the $\delta^{13}C$ values of *n*-alkanes, including: (a) $\delta^{13}C$ of organic matter source (organofacies), paleoenvironment, and organism physiology and metabolism; (b) $^{13}C/^{12}C$ fractionation during kerogen maturation; (c) $^{13}C/^{12}C$ kinetic fractionation on the expelled and migrating fluids and (d) reservoir filling history due to migration, biodegradation and mixing. Santos Neto et al. (1998), showed that the paleoenvironmental conditions of the Pendência and Alagamar Formations from the Potiguar Basin (Brazil) can be distinguished

Table 1
Basic geochemical parameters for the Mero Field crude oils.

Sample	Well A	Well B	Well C
% Saturates	44.21	53.54	50.49
% Aromatics	23.16	16.42	21.42
% NSO	32.63	30.04	28.09
$\delta^{13}C$ (‰)	−25.5	−25.7	−25.6
Pr/*n*-C_{17}	0.51	0.51	0.58
Ph/*n*-C_{18}	0.35	0.37	0.38
CPI	1.04	1.02	1.04
°API	27.53	28.19	27.79
Pr/Ph	1.97	1.80	1.89
HOP/STER	9.06	9.04	8.13
TRIC/HOP	0.39	0.37	0.40
H29/H30	0.56	0.55	0.57
GAM/H30	0.15	0.15	0.23
H35/H34	0.63	0.64	0.60
DIA/C27AA	0.56	0.54	0.58
TPP (*m*/*z* 259)	0.70	0.72	0.70
% 27 aßßR&S (218)	46.45	45.69	47.83
% 28 aßßR&S (218)	22.23	22.50	21.87
% 29 aßßR&S (218)	31.32	31.81	30.30
NORNEO/H29	0.18	0.17	0.17
DIAH/H30	0.04	0.04	0.05
DIA30/C27AA	0.69	0.75	0.87
TS/(TS + TM)	0.24	0.24	0.24
C29BB/C29	0.44	0.44	0.47
S/S + R	0.41	0.44	0.42
NOR25H/H30	0.13	0.13	0.13

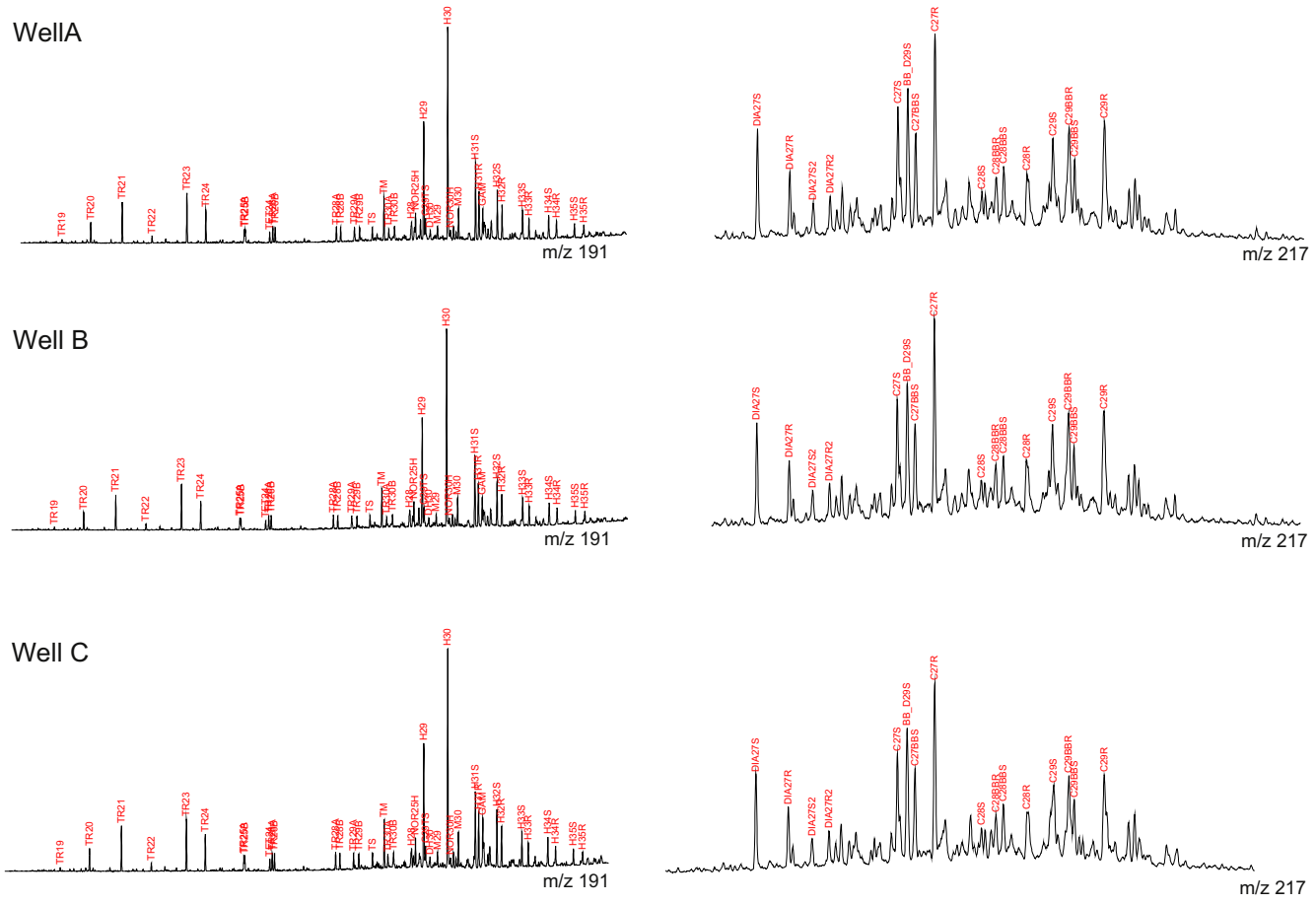

Fig. 3. Terpane distributions (*m/z* 191 – left) and steranes distrubtions (*m/z* 217 – right) of crude oils recovered from Mero Field.

by the isotopic composition of individual compounds. Guthrie et al. (1996) used compound-specific analyses (CSIA) of *n*-alkanes to differentiate extracts from a suite of organic-rich, immature shales from various basin in Brazil and observed that hydrocarbons from lacustrine shales are consistently more depleted in ^{13}C compared to marine shales. Murray et al. (1994) demonstrated that source matter type is clearly the primary factor determining the shape of the *n*-alkane isotope profile and the authors showed that marine oils display more commonly a flat or positively sloping profile.

For the three Mero Field samples, the similarity of the $\delta^{13}C$ whole oil values (−25.7‰ to −25.5‰) and distribution of $\delta^{13}C$ values for individual *n*-alkanes indicate that they were generated from the same source rock and generation pod. However, the $\delta^{13}C$ values for the *n*-alkanes show a larger variation from −29.1‰ to −24.9‰ with a remarkable "asymmetric U-shaped" isotope profile presence of lighter compounds in the range of C_{19}-C_{30} *n*-alkanes, showing an "asymmetric U-shaped" isotope profile (Fig. 4). According to Guzzo and Santos Neto (2006), this pattern is typical for Brazilian lacustrine oils.

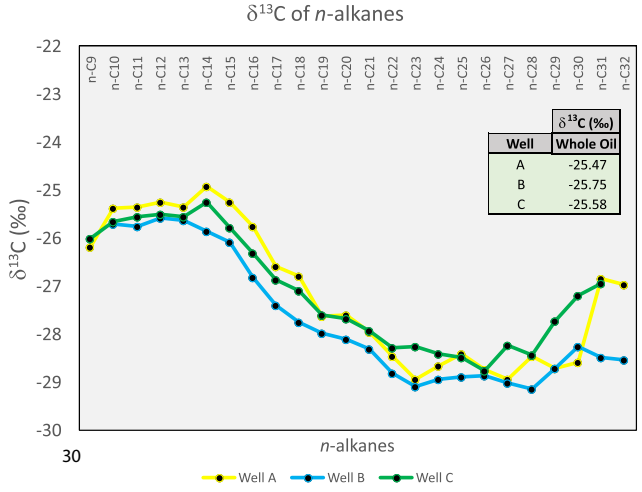

Fig. 4. Carbon isotope compositions of *n*-C_9 to *n*-C_{32} alkanes from Mero Field oil. The whole oil values are also highlighted.

4.2. Negative-ion ESI FT-ICR MS characterization

4.2.1. Heteroatomic class distributions

Heteroatomic compound classes N_1, N_1O_1, N_1O_2, N_1O_3, O_1, O_2, O_3S, and O_4S_1 were assigned in the Mero oil samples analyzed (Table 2). The lumped elemental class distributions of the oils show that the nitrogen containing species (Nx) and oxygen containing species (Oz) are the most abundant (70–80% of the total monoisotopic ion abundance) species, representing the acidic compound fraction of all assigned compounds in the samples. The less abundant species present are NxOz (ranging from 18% to 26%) and OxSy, which represented less than 10% of the total of assigned masses. The dominant Nx species comprises 45–50% of the Mero oils, followed by the Oz species that represents an average value of 28%. The distributions of the elemental classes between the analyzed oils were very similar suggesting that these oils are genetically related.

Table 2
Elemental and compound classes distributions for Mero Field crude oils.

	Elemental classes (%)				Compound classes distribution (%)							
Well	N_x	O_z	N_xO_z	O_zS_y	N	NO	NO_2	NO_3	O	O_2	O_4S	O_3S
Well A	45.2	26.2	25.6	3.0	45	14.8	9	2	10	16	3.0	
Well B	48.1	26.9	17.5	7.5	48	10.4	6	1	12	15	5.1	2.4
Well C	49.8	29.8	18.5	1.9	50	10.5	6	2	12	18	0.5	1.4

The dominant individual heteroatom class based on the relative abundance is N_1 (45–50% – average: 48%), followed by O_2 (15–18% – average: 16%), N_1O_1 (10–15% – average: 12%) and O_1 (10–12% – average: 11%) (Table 2). These findings are in agreement with previous studies that applied –ESI FT-ICR MS (Hughey et al., 2002; Cui et al., 2014; Mahlstedt et al., 2016; Wan et al., 2017; Rocha et al., 2018a), indicating a predominance of N_1 species in non-biodegraded crude oils.

The distribution of these major classes is shown in Fig. 5. Lacustrine oils tend to be enriched in N_1 compounds due to the relatively low content of Ox species derived from source rocks containing Type I kerogen (Wan et al., 2017; Ji et al., 2018; Rocha et al., 2018a). Recently, Ji et al. (2018) observed that the abundance of O_2 species in freshwater lacustrine oils, could be used as a tool to distinguish freshwater lacustrine oils from lacustrine saline oils.

4.2.2. Detailed characterization of the N_1 species

Pyrrolic nitrogen compounds significantly contribute to crude oil and bitumen (source rock) composition and are present in oils from different sources (marine and lacustrine facies). Previous studies have shown the formation of nitrogen compounds can be attributed to and origin from higher plants and blue-green algae, by formation during diagenesis (alkaloid), or by early diagenetic reactions of amino acids (Ji et al., 2018; and references therein).

The analyzed oils exhibit very similar double bound equivalent (DBE) and carbon number distributions of N_1 species. The DBE values ranged from 6 to 23 (mainly 9–18) and the carbon numbers ranged from 15 to 59 (mainly 20–44) – Fig. 6. The N_1 class is inferred to be dominated mostly by carbazoles (DBE 9), benzocarbazoles (DBE 12) and dibenzocarbazoles (DBE 15). This type of distribution pattern has been reported for several crude oils from different basins around the world (Oldenburg et al., 2014; Poetz et al., 2014; Mahlstedt et al., 2016; Wan et al., 2017; Han et al., 2018b; Rocha et al., 2018a).

An important variation in the N_1 class distributions of oils with similar origins has been reported as being a result of increasing thermal maturity. The increase in thermal maturity contributes to an increase in the aromatization/condensation (increased DBE values) associated with a decrease in the carbon number range of N_1, which indicates that substantial amounts of dealkylated species occur in the polar fraction as maturity increases (Oldenburg et al., 2014; Rocha et al., 2018b). Considering that the DBE and carbon number distribution for these oil samples are practically the same, we conclude that the Mero field's filling history included an oil charge derived from a single source facies at a similar level of thermal maturity. This is in consistent with the chemical kinetic characteristics of lacustrine Type I kerogen that has a narrow activation energy distribution and a homogeneous chemical bond structure (Min et al., 2011).

4.2.3. Detailed characterization of the O_1 class

The O_1 class species have a DBE distribution ranging from 4 to 17 (Fig. 7). The O_1 class species are more abundant at DBE 4 (22.4–23% – average: 22.7%) and DBE 5 (19.4–21.1% – average:

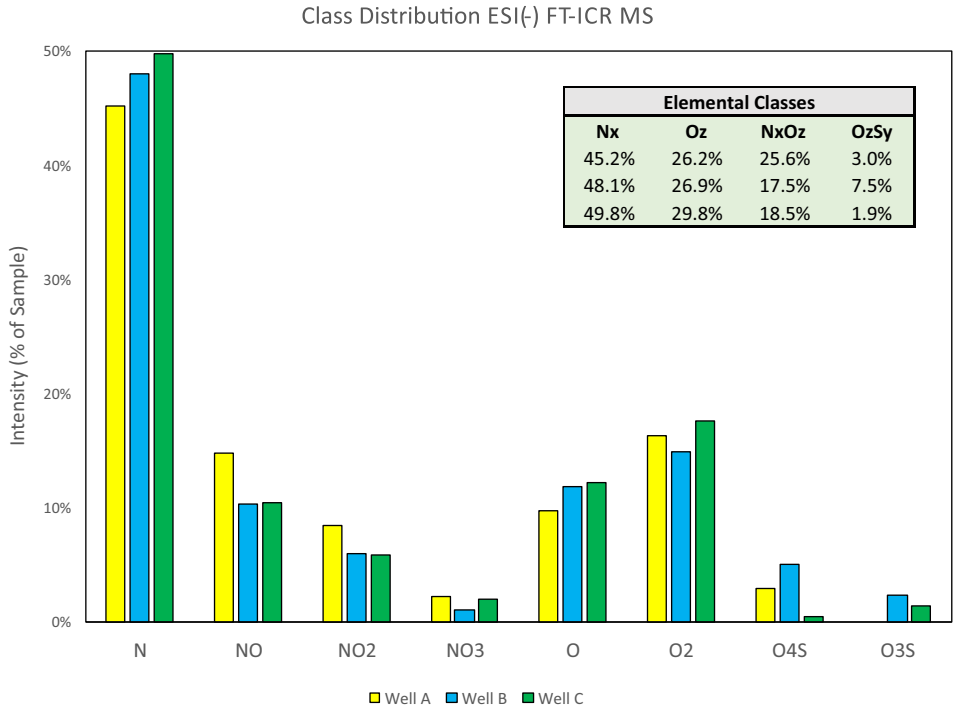

Fig. 5. Compound class distributions of crude oils recovered from Mero Field by ESI (–) FT-ICR MS. The elemental class distribution is highlighted.

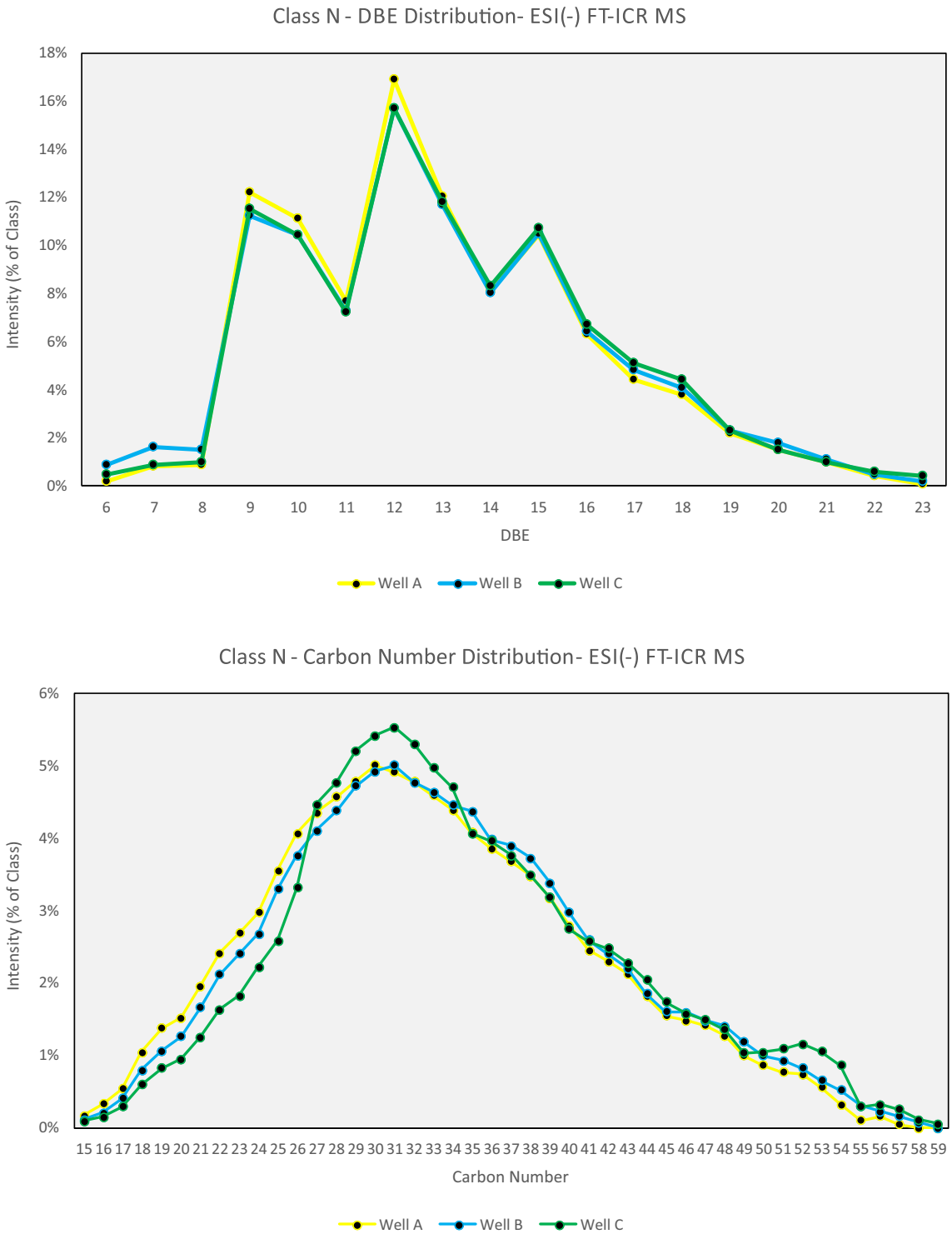

Fig. 6. Distribution of N_1-class measured in ESI negative ion mode. The upper plot shows the distributions of these molecular types, which are sorted into groups of double bond equivalent pseudohomologs (DBE) versus a "Percent of Class" plot (sum of the intensities of all components within one DBE group normalized to the sum of all assigned peak abundances of one heteroatom class measured in one ionization mode). The bottom plot shows the distribution of the N1-class sorted by the pseudohomolog carbon number C# versus the fraction of the total heteroatom class measured in the ESI negative ion mode.

20%). In addition, the relative abundance of the O_1 class species decreases gradually as the DBE value increases.

The O_1 class species are most likely components of a hydroxyl functional group that is deprotonated (Oldenburg et al., 2014) and is related to phenolic compounds (Shi et al., 2010). The occurrence of the O_1 class is commonly reported in crude oils and source rocks (Pereira et al., 2013; Vaz et al., 2013; Cui et al., 2014; Poetz et al., 2014; Mahlstedt et al., 2016; Oldenburg et al., 2017; Wan et al., 2017; Rocha et al., 2018a).

The carbon number distributions for O_1 class compounds with DBE 4 and DBE 5 show a normal distribution with a maxima in species with 27 and 28 carbon atoms, respective (Fig. 7). These compounds have been routinely reported in recent studies of crude oils using –ESI FT-ICR MS, thus indicating that sterols could occur

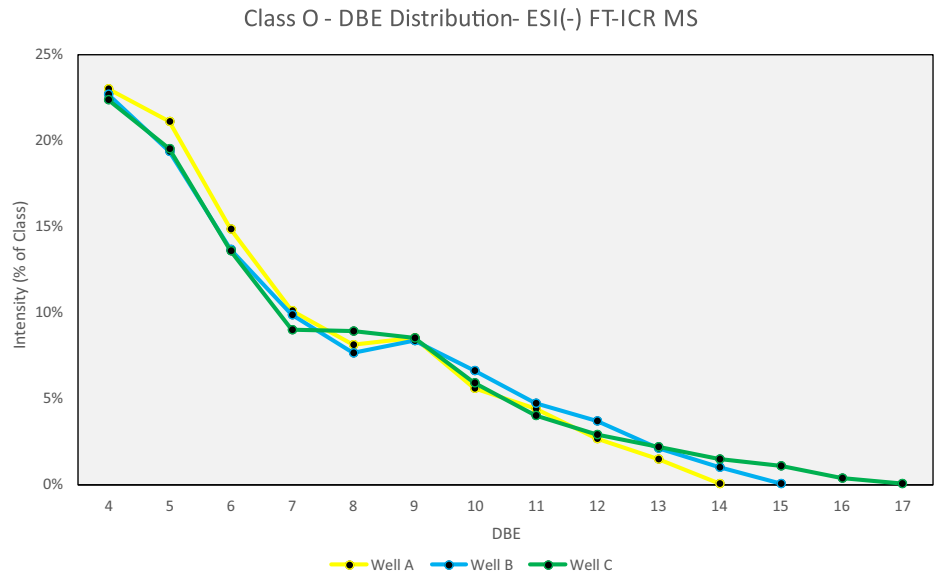

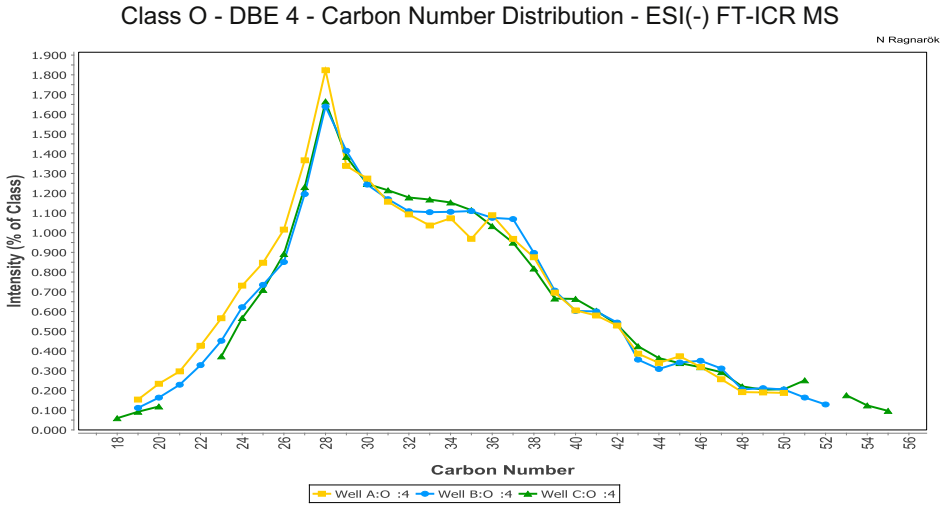

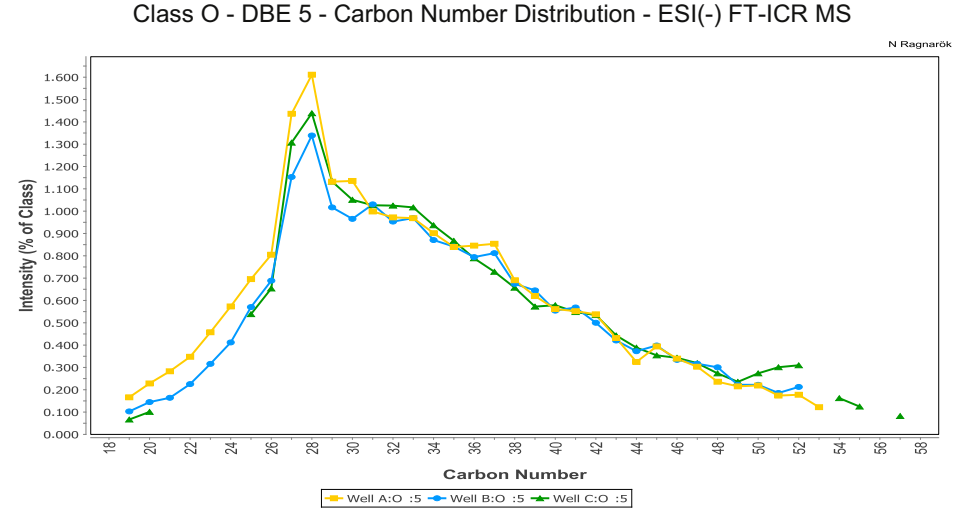

Fig. 7. The O_1-class distribution measured in the ESI negative ion mode. The upper plot shows the distributions of these molecular types, which are sorted into groups of double bond equivalent pseudohomologs (DBE) versus a "Percent of Class" plot (sum of the intensities of all components within one DBE group normalized to the sum of all assigned peak abundances of one (heteroatom) class measured in one ionization mode. The middle and bottom plots show the distributions of the DBE 4 and 5 compound groups of the O1-class sorted by pseudohomolog carbon number C# versus the fraction of the total heteroatom class measured in the ESI negative ion mode.

in crude oils (Shi et al., 2010; Oldenburg et al., 2014; Rocha et al., 2018a).

4.2.4. Detailed characterization of the O_2 class

The O_2 class species assigned from the crude oils have DBE values ranging from 1 to 15 (Fig. 8). Generally, there is a strong predominance of DBE 1 (17.3–25.9% – average: 20.6%), followed by an enrichment of DBE 5 (11.4–15.8% – average: 13%) and DBE 6 (8.8–12.2% – average: 10.2%). The O_2 class species detected by negative ESI FT-ICR MS could be attributed to carboxylic acids, and the O_2 class species with DBE 1 are considered as fatty acids (Kim et al., 2005; Li et al., 2010; Vaz et al., 2013; Wan et al., 2017). The DBE 5 and 6 of class O_2 can represent, steranoic and hopanoic acids, respectively.

4.2.5. Detailed characterization of the N_1O_1 class

The N_1O_1 class species are the most abundant NxOz compounds, ranging from 10.4% to 14.8% (Fig. 9). They show DBE values from 5 up to 25 (mainly 10–19), with maximum values at DBE 13, 14, 15 and 18. A previous study attempted to determine the exact structures of the N_1O_1 species, but more work is needed (Han et al., 2018a). Fluorenonocarbazoles were indicated as possible core structures for N_1O_1 classes DBE 15, 18 and 21 by Poetz et al. (2014). Recently, Han et al. (2018a) showed that the N_1O_1 class may share common formation precursors and mechanisms with the N_1 and N_2 compounds. Furthermore, the authors also proposed a schematic diagram to exemplify the possible evolution pathways to generate NxOz compounds from nonfluorescent chlorophyll catabolites (NCCs).

Rocha et al. (2018a) demonstrated that the N_1O_1 class may be used as a biomarker to distinguish the differences in the paleoenvironments of the deposition of organic matter between lacustrine and marine-derived oils. It is possible to clearly separate lacustrine and marine-derived oils due to the difference regarding the DBE values distribution observed. That difference occurs due to differences in kerogen type, that reflects the original biological sources and organic matter content, and with different degrees of aromatization and condensation of their constituents. The N_1O_1 class distribution for the Mero Field oils indicate a lacustrine source.

4.2.6. Organic sulfur compounds revealed by negative ESI FT-ICR MS

Liu et al. (2018) summarized the occurrence of organic sulfur compounds (OSCs) in immature sediments and crude oils and indicated that most of the sulfur in OSCs is originated by the incorporation of inorganic sulfides (H_2S, HS_x^-, and S_x^-) into functionalized hydrocarbons and carbohydrates during early diagenesis. These reactions might occur under specific conditions, such as an anoxic environment with low amounts of available ferric ions (Orr and Sinninghe Damsté, 1990). Weakly polar sulfur-containing compounds are, in general, not ionizable under ESI conditions without previous derivatization (Han et al., 2018).

In this work, the classes O_3S and O_4S were assigned in very low amounts (less than 2.5% for the O_3S and a ranging from 0.5% to 5.1% of O_4S compounds). A portion of these are attributed to contamination. The O_3S compounds refer to anions such as $C_{17}H_{27}O_3S^-$ (m/z 311.1685), $C_{18}H_{29}O_3S^-$ (m/z 325.1842) and $C_{19}H_{31}O_3S^-$ (m/z 339.1998) (Fig. 10). Melendez-Perez et al. (2016) stated that these compounds are alkylbenzene sulfonates, compounds that are anionic surfactants and are among the most widely used surfactants in domestic detergents. Therefore, this class will not be used for any interpretation since it may represent a contamination of the samples.

5. Geochemical characterization of polar compounds to assess source and thermal maturity

5.1. Maturity assessment

Several studies have recognized new parameters to evaluate the thermal evolution of crude oils using ratios obtained by –ESI FT-ICR MS (Oldenburg et al., 2014; Poetz et al., 2014; Wan et al., 2017; Ji et al., 2018; Rocha et al., 2018b). These new parameters have been shown to be a useful tools for maturity assessment, and may help resolve maturity variations across the oil window. Some of these parameters have the advantage of being directly linked to vitrinite

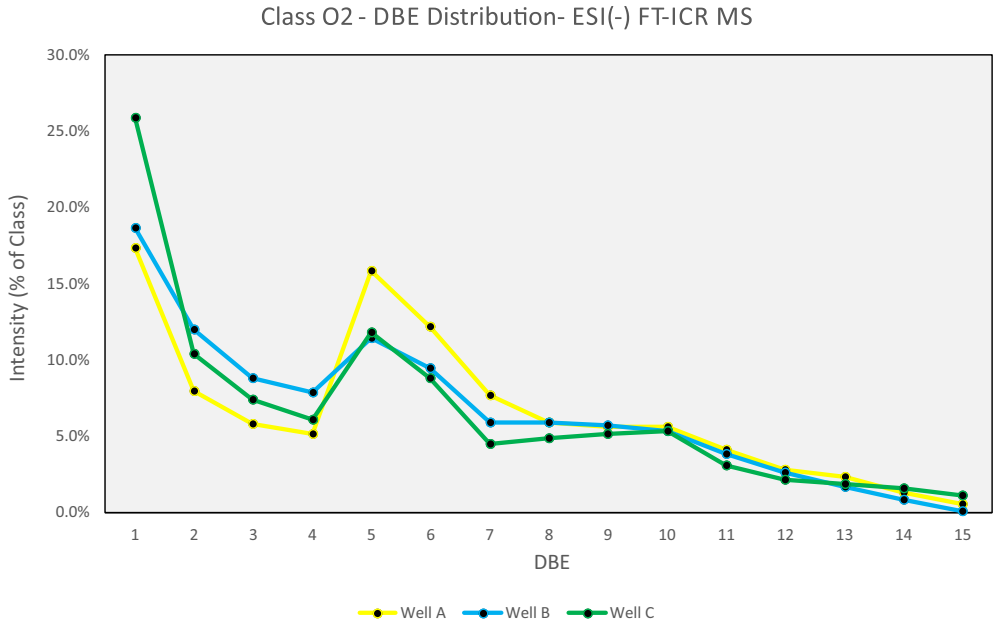

Fig. 8. Distribution of O_2-class measured in the ESI negative ion mode. The plot shows the distributions of these molecular types, which are sorted into groups of double bond equivalent pseudohomologs (DBE) versus a "Percent of Class" plot (sum of the intensities of all components within one DBE group normalized to the sum of all assigned peak abundances of one heteroatom class measured in one ionization mode).

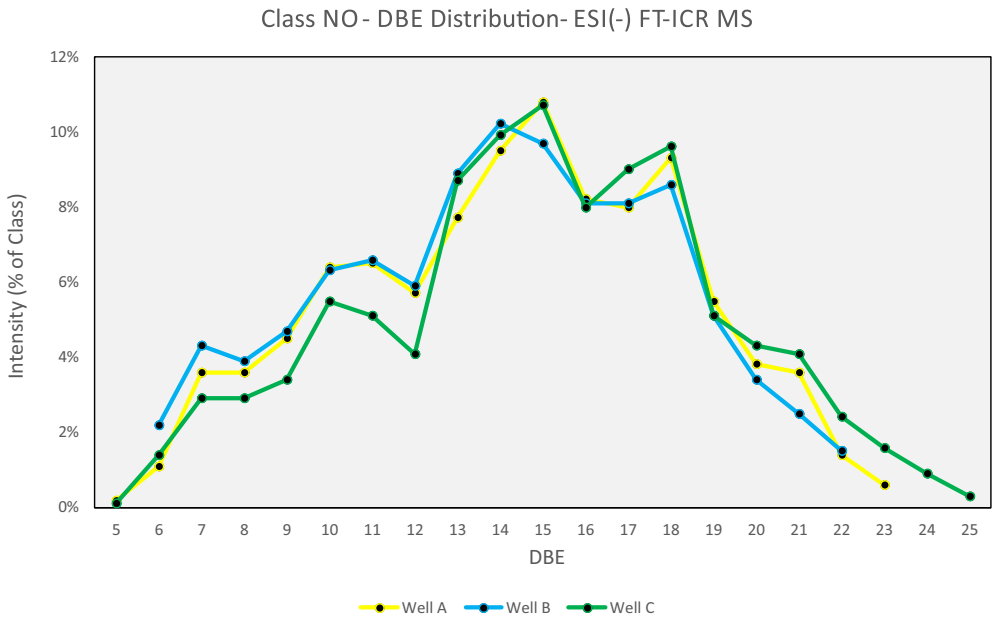

Fig. 9. Distribution of the N_1O_1-class measured in the ESI negative ion mode. The plot shows the distributions of these molecular types, sorted into groups of double bond equivalent pseudohomologs (DBE) versus a "Percent of Class" plot (sum of the intensities of all components within one DBE group normalized to the sum of all assigned peak abundances of one heteroatom class measured in one ionization mode).

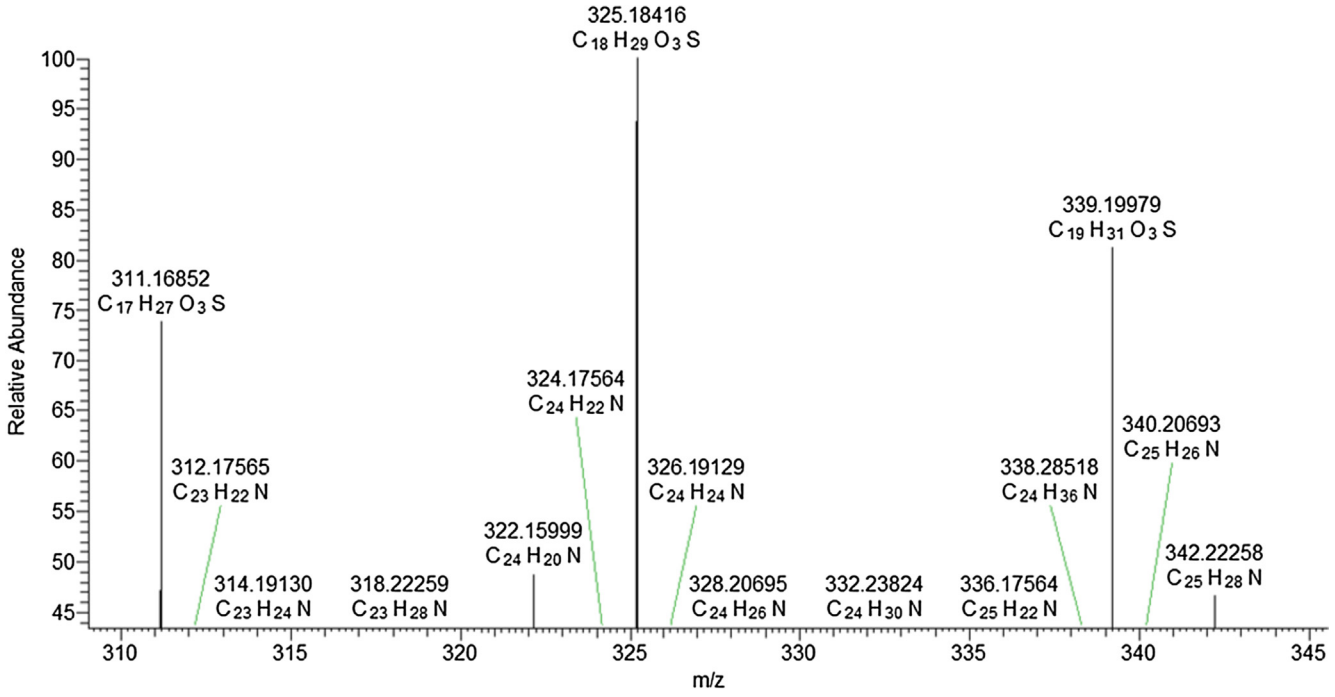

Fig. 10. ESI(-) FT-ICM MS showing O_3S compounds related to alkylbenzene sulfonates: $C_{17}H_{27}O_3S-$ (*m/z* 311.1685), $C18H_{29}O_3S-$ (*m/z* 325.1842) and $C_{19}H_{31}O_3S$ – (*m/z* 339.1998).

reflectance while others are more qualitative, such as indicating relative maturity as "low-mature oil", "mature oil" or "highly-mature oil".

For thermal maturity assessment, a triangular diagram showing relative changes of the three major compound groups of N_1 class species – such as carbazoles (DBE 9), benzocarbazoles (DBE 12) and dibenzocarbazoles (DBE 15) – as proposed by Oldenburg et al. (2014) was applied. These authors studied North Sea crude oils that belong to one single petroleum family generated predominantly from the Upper Jurassic Kimmeridge Clay Formation (Bennett et al., 2002). This formation was deposited under anoxic or dysaerobic conditions in a stratified shelf sea, with a predominance of a Type II kerogen (Scotchman, 1991). Additionally, a regression obtained by Rocha et al. (2018b) was employed. The regression involves the relationship between the sum of the relative abundance of Class O_2 DBE values that increased versus the one that decreased with the ongoing maturity of the HP experiments. The HP experiments were conducted by Spigolon

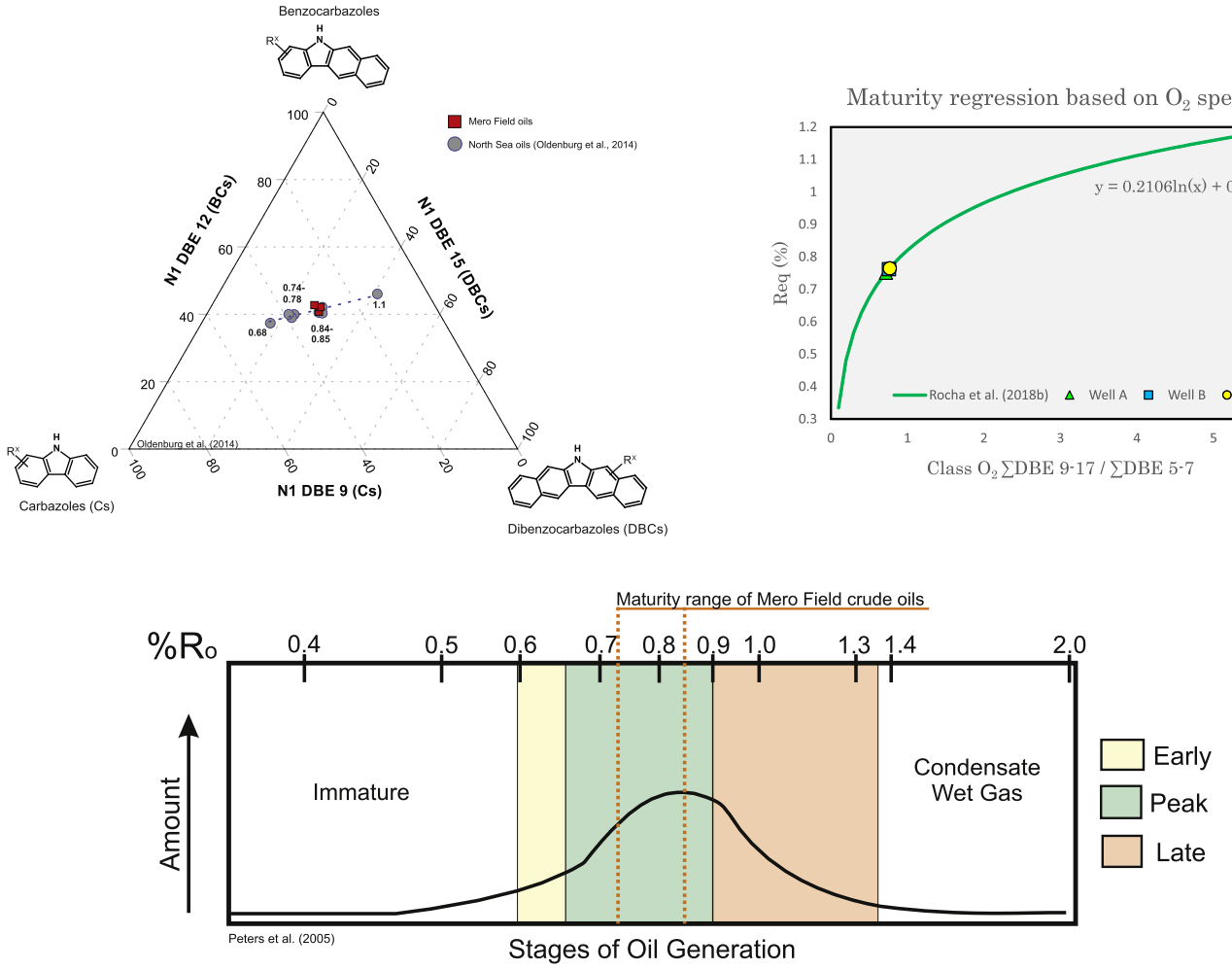

Fig. 11. Maturity assessment based on polar compounds. The crude oils recovered from Mero Field were generated under a thermal condition related to the peak of oil generation.

et al. (2015) and the authors used a source rock with a Type I kerogen.

The results are summarized in Fig. 11. Based on maturity assessment approaches using selected N_1 and O_2 species, the maturity degree corresponds to 0.84–0.85 %Ro and 0.72–0.77 %Ro, respectively.

5.2. Origin of the crude oils

The ability to distinguish crude oils from different origins using FT-ICR MS has been demonstrated in previous studies (e.g., Hughey et al., 2002; Wan et al., 2017; Rocha et al., 2018a). This ability is possible because both the concentration and the distribution of heteroatomic compounds vary according to the geological origins of the oils from related source rocks (Rocha et al., 2018a). Based on these results a paleoenvironmental assessment of the crude oil samples was performed in this study.

In this work, we applied the ratios, defined by Rocha et al. (2018a), designed for the geochemical characterization of the crude oils. The results indicate that the Mero Field crude oils were generated by a source rock that was deposited in a lacustrine environment (Fig. 12). Using the stratigraphic sequence and sedimentology context of the pre-salt, it is likely that the Itapema Formation (Jiquiá stage) was the source rock for those oils.

6. Conclusions

Eight different heteroatomic classes were detected in three Mero Field crude oil samples by negative ESI FT-ICR-MS analysis. This technique allows a molecular-level analysis of complex mixtures with accurate mass measurements and provides unique information on elemental compositions for these oils. We clearly demonstrate that –ESI FT-ICR MS is a reliable and valuable tool for performing geochemical assessments, as it allows for a full comprehension of crude oil composition and obtains information about origin and maturity parameters.

Based on their relative ion abundance, the N_1 species are the dominant heteroatomic class, followed by the O_2, N_1O_1, and O_1 classes. Similar class distributions have been attributed to lacustrine oils that show a tendency to be enriched in nitrogen-containing compounds.

The DBE and carbon number distributions for the N_1, O_1 and O_2 classes are nearly identical. These findings indicate that Mero's Field experienced an oil charge from the same source at the thermal maturity conditions.

The maturity assessment of Mero oils was made using a triangular diagram created by Oldenburg et al. (2014) associated with a regression obtained by Rocha et al. (2018b). The results point to a maturity level correlated to the peak of oil generation (0.7–0.9%Ro).

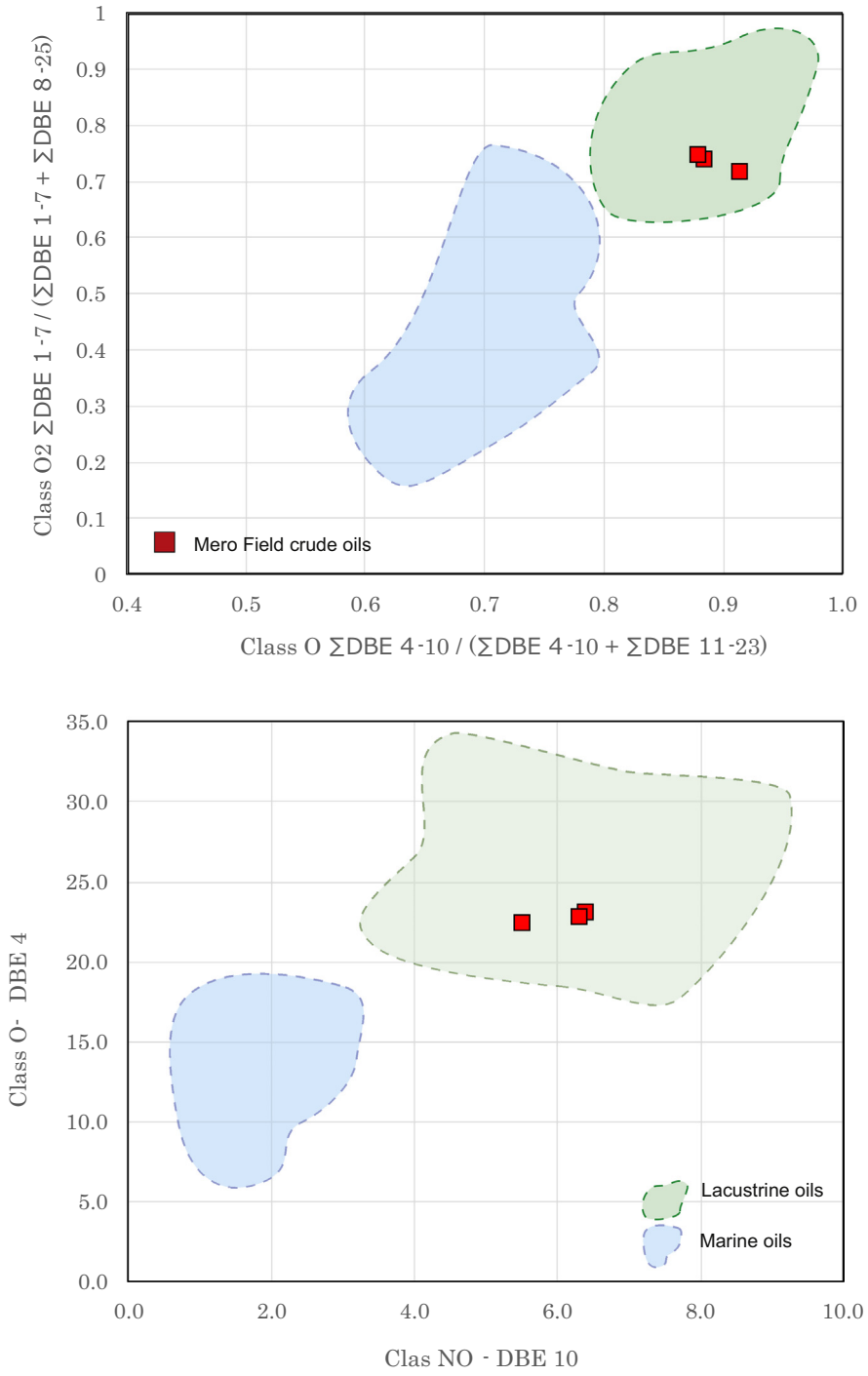

Fig. 12. Depositional environment assessment of crude oils from the Mero Field based on the distribution of polar compounds.

The source-rock paleoenvironmental conditions is inferred to be lacustrine based on several ratios from Rocha et al. (2018b).

Acknowledgments

The financial support provided by Petrobras – Petróleo Brasileiro SA is appreciated. The authors are grateful to the Geochemistry Lab staff at the Petrobras Research and Development Center (CENPES) and the ThoMSon Laboratory (UNICAMP) team. We thank the Associate Editor Clifford C. Walters, John Guthrie and an anonymous reviewer for critical comments, which helped us to improve the manuscript. We also thank Mario Rangel, Alexandre Ferreira, Wagner Bastos, Fabiano Leal and Mônica Rocha for providing useful suggestions.

Associate Editor—**Clifford C. Walters**

References

Bennett, B., Chen, M., Brincat, D., Gelin, F.J.P., Larter, S.R., 2002. Fractionation of benzocarbazoles between source rocks and petroleums. Organic Geochemistry 33, 545–559.

Carlotto, M.A., Silva, R.C.B. da, Yamato, A.A., Trindade, W.L., Moreira, J.L.P., Fernandes, R.A.R., Ribeiro, O.J.S., Gouveia Jr., W.P., Carminati, J.P., Qicai, D., Junfeng, Z., Silva-Teles Jr., A.C. da, 2017. Libra: A newborn giant in the Brazilian

Presalt Province. In: Merrill, R.K., Sternbach, C.A. (Eds.) Giant Fields of the Decade 2000–2010, American Association of Petroleum Geologists Memoir 113, Tulsa, pp. 165–176.
Chaboureau, A.C., Guillocheau, F., Robin, C., Rohais, S., Moulin, M., Aslanian, D., 2013. Paleogeographic evolution of the central segment of the South Atlantic during Early Cretaceous times: paleotopographic and geodynamic implications. Tectonophysics 604, 191–223.
Chafetz, H., Barth, J., Cook, M., Guo, X., Zhou, J., 2018. Origins of carbonate spherulites: implications for Brazilian Aptian pre-salt reservoir. Sedimentary Geology 365, 21–33.
Cui, J., Zhu, R., Hu, J., 2014. Identification and geochemical significance of polarized macromolecular compounds in lacustrine and marine oils. Chinese Journal of Geochemistry 33, 431–438.
Dembicki, H., 2016. Practical Petroleum Geochemistry for Exploration and Production. Elsevier, 342 pp
Guthrie, J.M., Trindade, L.A.F., Eckardt, C.B., Takaki, T., 1996. Molecular and carbon isotopic analysis of specific biological markers: evidence for distinguishing between marine and lacustrine depositional environments in sedimentary basins of Brazil. American Association of Petroleum Geologists Annual Convention, San Diego, CA, Abstract, A-58.
Guzzo, J.V.P., Santos Neto, E.V., 2006. Stables carbon isotopic fingerprints of individual n-alkanes in Brazilian oils. In: 10th ALAGO Congress on Organic Geochemistry. Salvador, BA, Brazil.
Han, Y., Poetz, S., Mahlstedt, N., Karger, C., Horsfield, B., 2018a. Fractionation and origin of NyOxand Oxcompounds in the Barnett Shale sequence of the Marathon 1 Mesquite well, Texas. Marine and Petroleum Geology 97, 517–524.
Han, Y., Poetz, S., Mahlstedt, N., Karger, C., Horsfield, B., 2018b. Fractionation of pyrrolic nitrogen compounds during primary migration of petroleum within the Barnett Shale Sequence of Marathon 1 Mesquite Well, Texas. Energy & Fuels 32, 4638–4650.
Han, Y., Zhang, Y., Xu, C., Hsu, C.S., 2018c. Molecular characterization of sulfur-containing compounds in petroleum. Fuel 221, 144–158.
Hughey, C.A., Rodgers, R.P., Marshall, A.G., Qian, K., Robbins, W.K., 2002. Identification of acidic NSO compounds in crude oils of different gochemical origins by negative-ion electrospray Fourier transform ion cyclotron resonance mass spectrometry. Organic Geochemistry 33, 743–759.
Hughey, C.A., Rodgers, R.P., Marshall, A.G., Walters, C.C., Qian, K., Mankiewicz, P., 2004. Acidic and neutral polar NSO compounds in Smackover oils of different thermal maturity revealed by electrospray high field Fourier transform ion cyclotron resonance mass spectrometry. Organic Geochemistry 35, 863–880.
Ji, H., Li, S., Greenwood, P., Zhang, H., Pang, X., Xu, T., He, N., Shi, Q., 2018. Geochemical characteristics and significance of heteroatom compounds in lacustrine oils of the Dongpu Depression (Bohai Bay Basin, China) by negative-ion Fourier transform ion cyclotron resonance mass spectrometry. Marine and Petroleum Geology 97, 568–591.
Kim, S., Stanford, L.A., Rodgers, R.P., Marshall, A.G., Walters, C.C., Qian, K., Wenger, L. M., Mankiewicz, P., 2005. Microbial alteration of the acidic and neutral polar NSO compounds revealed by Fourier transform ion cyclotron resonance mass spectrometry. Organic Geochemistry 36, 1117–1134.
Li, M., Cheng, D., Pan, X., Dou, L., Hou, D., Shi, Q., Wen, Z., Tang, Y., Achal, S., Milovic, M., Tremblay, L., 2010. Characterization of petroleum acids using combined FT-IR, FT-ICR-MS and GC-MS: implications for the origin of high acidity oils in the Muglad Basin, Sudan. Organic Geochemistry 41, 959–965.
Liu, W., Liao, Y., Shi, Q., Hsu, C.S., Jiang, B., Peng, P., 2018. Origin of polar organic sulfur compounds in immature crude oils revealed by ESI FT-ICR MS. Organic Geochemistry 121, 36–47.
Mahlstedt, N., Horsfield, B., Wilkes, H., Poetz, S., 2016. Tracing the impact of fluid retention on bulk petroleum properties using nitrogen-containing compounds. Energy & Fuels 30, 6290–6305.
Marshall, A.G., Hendrickson, C.L., Emmett, M.R., Rodgers, R.P., Blakney, G.T., Nilsson, C.L., 2007. Fourier transform ion cyclotron resonance: state of the art. European Journal of Mass Spectrometry 13, 57–59.
Marshall, A.G., Rodgers, R.P., 2004. Petroleomics: the next grand challenge for chemical analysis. Accounts of Chemical Research 37, 53–59.
Melendez-Perez, J.J., Martínez-Mejía, M.J., Awan, A.T., Fadini, P.S., Mozeto, A.A., Eberlin, M.N., 2016. Characterization and comparison of riverine, lacustrine, marine and estuarine dissolved organic matter by ultra-high resolution and accuracy Fourier transform mass spectrometry. Organic Geochemistry 101, 99–107.
Mello, M.R., Gaglianone, P.C., Brassell, S.C., Maxwell, J.R., 1988. Geochemical and biological marker assessment of depositional environments using Brazilian offshore oils. Marine and Petroleum Geology 5, 205–223.
Min, W., Shuang-fang, L., Hai-tao, X., 2011. Kinetic simulation of hydrocarbon generation from lacustrine type I kerogen from the Songliao Basin: model comparison and geological application. Marine and Petroleum Geology 28, 1714–1726.
Moreira, J.L.P., Madeira, C.V., Gil, J.A., Machado, M.A.P., 2007. Santos Basin|Bacia de Santos. Boletim de Geociências da Petrobras 15, 531–549.
Murray, A.P., Summons, R.E., Boreham, C.J., Dowling, L.M., 1994. Biomarker and nalkane isotope profiles for Tertiary oils: relationship to source rock depositional setting. Organic Geochemistry 22, 521–542.
Oldenburg, T.B.P., Brown, M., Bennett, B., Larter, S.R., 2014. The impact of thermal maturity level on the composition of crude oils, assessed using ultra-high resolution mass spectrometry. Organic Geochemistry 75, 151–168.
Oldenburg, T.B.P., Jones, M., Huang, H., Bennett, B., Shafiee, N.S., Head, I., Larter, S.R., 2017. The controls on the composition of biodegraded oils in the deep subsurface – Part 4. Destruction and production of high molecular weight non-hydrocarbon species and destruction of aromatic hydrocarbons during progressive in-reservoir biodegradation. Organic Geochemistry 114, 57–80.
Orr, W.L., Sinninghe Damsté, J.S., 1990. Geochemistry of sulfur in petroleum systems. In: Orr, W.L., White, C.M. (Eds.) Geochemistry of Sulfur in Fossil Fuels, ACS Symposium Series. American Chemical Society, pp. 2–29.
Pedentchouk, N., Turich, C., 2017. Carbon and hydrogen isotopic compositions of *n*-alkanes as a tool in petroleum exploration. Geological Society, London, Special Publications 468, 105–125.
Pereira, R.C.L., Simas, R.C., Corilo, Y.E., Vaz, B.G., Klitzke, C.F., Schmidt, E.M., Pudenzi, M.A., Silva, R.M.C.F., Moraes, E.T., Bastos, W.L., Eberlin, M.N., Nascimento, H.D.L., 2013. Precision in petroleomics via ultrahigh resolution electrospray ionization Fourier transform ion cyclotron resonance mass spectrometry. Energy & Fuels 27, 7208–7216.
Peters, K.E., Walters, C.C., Moldowan, J.M., 2005. The Biomarker Guide. Cambridge University Press, p. 1155 pp.
Pietzsch, R., Oliveira, D.M., Tedeschi, L.R., Queiroz Neto, J.V., Figueiredo, M.F., Vazquez, J.C., de Souza, R.S., 2018. Palaeohydrology of the Lower Cretaceous pre-salt lacustrine system, from rift to post-rift phase, Santos Basin, Brazil. Palaeogeography, Palaeoclimatology, Palaeoecology 507, 60–80.
Poetz, S., Horsfield, B., Wilkes, H., 2014. Maturity-driven generation and transformation of acidic compounds in the organic-rich Posidonia Shale as revealed by electrospray ionization Fourier transform ion cyclotron resonance mass spectrometry. Energy & Fuels 28, 4877–4888.
Qian, K., Rodgers, R.P., Hendrickson, C.L., Emmett, M.R., Marshall, A.G., 2001. Reading chemical fine print: resolution and identification of 3000 nitrogen-containing aromatic compounds from a single electrospray ionization Fourier transform ion cyclotron resonance mass spectrum of heavy petroleum crude oil. Energy & Fuels 15, 492–498.
Rocha, Y., dos, S., Pereira, R.C.L., Mendonça Filho, J.G., 2018a. Geochemical characterization of lacustrine and marine oils from off-shore Brazilian sedimentary basins using negative-ion electrospray Fourier transform ion cyclotron resonance mass spectrometry (ESI FTICR-MS). Organic Geochemistry 124, 29–45.
Rocha, Y., dos, S., Pereira, R.C.L., Mendonça Filho, J.G., 2018b. Negative electrospray Fourier transform ion cyclotron resonance mass spectrometry determination of the effects on the distribution of acids and nitrogen-containing compounds in the simulated thermal evolution of a Type-I source rock. Organic Geochemistry 115, 32–45.
Rodgers, R.P., Schaub, T.M., Marshall, A.G., 2005. Petroleomics: MS returns to its roots. Analytical Chemistry 77, 20 A–27 A.
Santos Neto, E.V., Hayes, J.M., Takaki, T., 1998. Isotopic biogeochemistry of the Neocomian lacustrine and upper Aptian marine-evaporitic sediments of the Potiguar Basin, northeastern Brazil. Organic Geochemistry 28, 361–381.
Scotchman, I.C., 1991. Kerogen facies and maturity of the Kimmeridge Clay Formation in southern and eastern England. Marine and Petroleum Geology 8, 278–295.
Shi, Q., Zhao, S., Xu, Z., Chung, K.H., Zhang, Y., Xu, C., 2010. Distribution of acids and neutral nitrogen compounds in a Chinese crude oil and its fractions: characterized by negative-ion electrospray ionization Fourier transform ion cyclotron resonance mass spectrometry. Energy & Fuels 24, 4005–4011.
Smith, D.F., Podgorski, D.C., Rodgers, R.P., Blakney, G.T., Hendrickson, C.L., 2018. 21 Tesla FT-ICR mass spectrometer for ultrahigh-resolution analysis of complex organic mixtures. Analytical Chemistry 90, 2041–2047.
Spigolon, A.L.D., Lewan, M.D., de Barros Penteado, H.L., Coutinho, L.F.C., Mendonça Filho, J.G., 2015. Evaluation of the petroleum composition and quality with increasing thermal maturity as simulated by hydrous pyrolysis: a case study using a Brazilian source rock with Type I kerogen. Organic Geochemistry 83–84, 27–53.
Tedeschi, L.R., Jenkyns, H.C., Robinson, S.A., Sanjinés, A.E.S., Viviers, M.C., Quintaes, C.M.S.P., Vazquez, J.C., 2017. New age constraints on Aptian evaporites and carbonates from the South Atlantic: implications for Oceanic Anoxic Event 1a. Geology 45, 543–546.
Vaz, B.G., Silva, R.C., Klitzke, C.F., Simas, R.C., Lopes Nascimento, H.D., Pereira, R.C.L., Garcia, D.F., Eberlin, M.N., Azevedo, D.A., 2013. Assessing biodegradation in the llanos orientales crude oils by electrospray ionization ultrahigh resolution and accuracy fourier transform mass spectrometry and chemometric analysis. Energy & Fuels 27, 1277–1284.
Wan, Z., Li, S., Pang, X., Dong, Y., Wang, Z., Chen, X., Meng, X., Shi, Q., 2017. Characteristics and geochemical significance of heteroatom compounds in terrestrial oils by negative-ion electrospray Fourier transform ion cyclotron resonance mass spectrometry. Organic Geochemistry 111, 34–55.
Ziegs, V., Noah, M., Poetz, S., Horsfield, B., Hartwig, A., Rinna, J., Skeie, J.E., 2018. Unravelling maturity- and migration-related carbazole and phenol distributions in Central Graben crude oils. Marine and Petroleum Geology 94, 114–130.